Simulation study of the influence of different gas puffing location on Z_{eff} for CFETR

M.Y. Ye, Y.F. Zhou, S.F. Mao

Department of Engineering and Applied Physics, University of Science and Technology of China, Hefei, China

In the future fusion reactor, power exhaust is one of the most critical issues due to the limit of the heat load onto divertor targets. Because the carbon are not suitable to be used as the first wall material, tungsten divertor is considered as the most appropriate candidate, which implies that impurity seeding is indispensable to mitigate heat load onto the divertor target via radiation. For CFETR phase II [1], the fusion power is designed up to 1 GW, a large radiation fraction is required to dissipate the heat power entering the scrape-off layer (SOL). Therefore, considerable amount of impurities would be seeded into the plasma. However, to avoid significant degradation of the main plasma, the impurity concentration should be kept at low level. To find an appropriate impurity seeding scheme for CFETR, lots of works are carried out [2,3]. In this paper, we focus on the influence of the gas puffing location on the effective ion charge Z_{eff}. With the argon impurity and fixed radiation fraction ~ 85%, SOLPS simulations are performed for four different gas puffing schemes: (1) deuterium and impurity mixed gas injected from the outer leg (OL), (2) mixed gas injected from the inner leg (IL), (3) mixed gas injected from the top of main chamber (UP) and (4) deuterium injected from the top while impurity injected from the outer leg (UO). The simulated results are compared in terms of radiative efficiency for different plasma densities. Furthermore, according to the Matthews' law [4], the simulated results are fitted to give the relationship between Z_{eff} and plasma density, which could provide the boundary condition for further optimization of the performance of the core plasma [5].

1. Simulation settings

The simulations for CFETR were performed using SOLPS5.0 code package [6], which includes the fluid plasma code B2.5 and the Monte-Carlo neutral transport code Eirene [7]. Geometry configuration and computational mesh using in SOLPS simulations is shown in Fig. 1, as well as the locations of pumping and gas puffing. The equilibrium is based on the preliminary design for CFETR using OMFIT framework [8]. Deuterium, helium and the seeded argon impurity are included in simulations, and wall sputtering is not considered in simulations. The recycling rates at first walls and divertor targets is fixed to 100% for all species, except for the location of pumping.

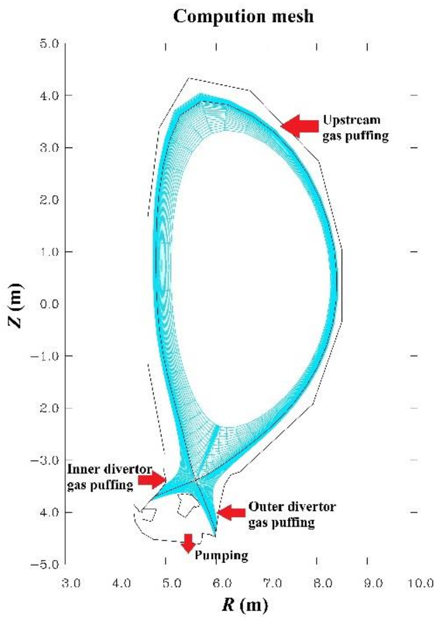

Fig. 1 The computation mesh and gas puffing locations.

The total power across the core-edge boundary (ρ = 0.9) P_{tot} is fixed to 200 MW and equally distributes to ions and electrons. A high radiation fraction $f_{\mathrm{rad}}^{\mathrm{edge}} = P_{\mathrm{rad}}^{\mathrm{edge}} / P_{\mathrm{tot}} \sim 0.85 \pm 0.02$ which results in a fully detached divertor regime is achieved in simulations by injecting deuterium gas and different impurity gases from different gas puffing locations. A density scan is performed by varying the deuterium ion density at the core-edge boundary in the range from 6.0×10^{19} m^{-3} to 1.0×10^{20} m^{-3}. A specific set of radially varying cross-field transport coefficients is identical for all ions account for the pedestal structure predicted by EPED model for CFETR H-mode discharges, is shown in Fig. 2.

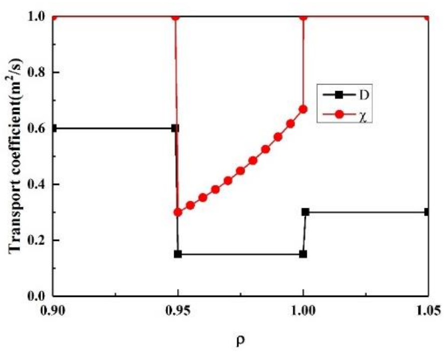

Fig. 2 Particle diffusivities *D* and thermal diffusivities χ at outer mid-plane.

2. Results and discussion

In order to figure out which of the seeding techniques is better, a radiative efficiency $H(Z_{eff})$ is defined as a ratio of the radiation fraction f_{rad}^{edge} to the increment Z_{eff} from simulation results:

$$H(Z_{eff}) = f_{rad}^{edge} / [Z_{eff} - 1] \quad (1).$$

As shown in Fig. 3, the upstream gas puffing case is related to the highest $H(Z_{eff})$ in the three mixed gas puffing cases. The benefit of the upstream gas puffing is mainly due to the larger SOL D^+ flux, which dominates the discrepancies of the divertor impurity screening in these cases. Furthermore, it can be seen that there is only a little improvement of $H(Z_{eff})$ for the UO case than the UP case, which implies that the impurity seeding locations only slightly influence the $H(Z_{eff})$. This result is similar to the experimental observations on C-Mod, in which it was found that the screening effects of recycling impurities are independent of impurity gas launch locations [9], because the major impurity sources will be the recycling sources of two divertor targets under a radiated fraction ~ 0.85.

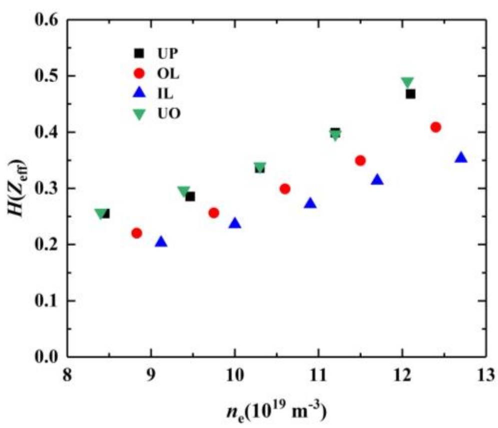

Fig. 3 The radiative efficiency for different puffing locations with different core-edge boundary electron density.

The Z_{eff} depends primarily on the electron density n_e and the radiated power P_{rad}, namely $(Z_{eff}-1) \propto P_{rad}/n_e^2$ according to a scaling from multi-machine database [4]. Based on this form the simulated Z_{eff} for argon seeding is fitted as

$$Z_{eff} = 1 + (1.71179 P_{rad})/n_e^2 \quad (2).$$

3. Conclusions

For the purpose of finding an appropriate impurity seeding scheme, the influence of the gas puffing location on the Z_{eff} under a high radiation fraction (~85%) is studied by SOLPS simulation. Four different gas puffing schemes are considered: (1) deuterium and argon mixed gas injected from the outer leg (OL), (2) mixed gas injected from the inner leg (IL), (3) mixed gas injected from the top of main chamber (UP) and (4) deuterium injected from the top while argon injected from the outer leg (UO). It is found that the UO scheme has the best radiative efficiency, and the puffing location of recycling impurities has a minor influence compared with the deuterium puffing location. Furthermore, the simulation results are fitted to the Matthews' law to give the relationship between the Z_{eff} and the plasma density, which is considered to provide the boundary condition for further optimization of the performance of the core plasma.

References

[1] Y.X. Wan, et al., Nucl. Fusion 57 (2017) 102009.

[2] M.Y. Ye, et al., Nucl. Fusion doi: 10.1088/1741-4326/ab2bd0, 2019.

[3] Y.F. Zhou, et al., Fus. Eng. Des. 136 (2018) 931.

[4] G. F. Matthews, et al, J. Nucl. Mater. 241-243 (1997) 450.

[5] N. Shi, et al, Nucl. Fusion 57 (2017) 126046

[6] R. Schneider R, et al., Contrib. Plasma Phys. 46 (2006) 3.

[7] D. Reiter, et al., Fusion Sci. Technol. 47 (2005) 172.

[8] O. Meneghini, L. Lao, Plasma and Fusion Research 8 (2013) 2403009.

[9] G.M. McCracken, et al., J. Nucl. Mater. 241-243 (1997) 777.